REVIEW SUMMARY

MEMBRANES

Maximizing the right stuff: The trade-off between membrane permeability and selectivity

Ho Bum Park, Jovan Kamcev, Lloyd M. Robeson, Menachem Elimelech, Benny D. Freeman*

BACKGROUND: Synthetic membranes are used for desalination, dialysis, sterile filtration, food processing, dehydration of air and other industrial, medical, and environmental applications due to low energy requirements, compact design, and mechanical simplicity. New applications are emerging from the water-energy nexus, shale gas extraction, and environmental needs such as carbon capture. All membranes exhibit a trade-off between permeability—i.e., how fast molecules pass through a membrane material—and selectivity—i.e., to what extent the desired molecules are separated from the rest. However, biological membranes such as aquaporins and ion channels are both highly permeable and highly selective. Separation based on size difference is common, but there are other ways to either block one component or enhance transport of another through a membrane. Based on increasing molecular understanding of both biological and synthetic membranes, key design criteria for new membranes have emerged: (i) properly sized free-volume elements (or pores), (ii) narrow free-volume element (or pore size) distribution, (iii) a thin active layer, and (iv) highly tuned interactions between permeants of interest and the membrane. Here, we discuss the permeability/selectivity trade-off, highlight similarities and differences between synthetic and biological membranes, describe challenges for existing membranes, and identify fruitful areas of future research.

ADVANCES: Many organic, inorganic, and hybrid materials have emerged as potential membranes. In addition to polymers, used for most membranes today, materials such as carbon molecular sieves, ceramics, zeolites, various nanomaterials (e.g., graphene, graphene oxide, and metal organic frameworks), and their mixtures with polymers have been explored. Simultaneously, global challenges such as climate change and rapid population growth stimulate the search for efficient water purification and energy-generation technologies, many of which are membrane-based. Additional driving forces include wastewater reuse from shale gas extraction and improvement of chemical and petrochemical separation processes by increasing the use of light hydrocarbons for chemicals manufacturing.

ON OUR WEBSITE

Read the full article at http://dx.doi.org/10.1126/science.aab0530

OUTLOOK: Opportunities for advancing membranes include (i) more mechanically, chemically, and thermally robust materials; (ii) judiciously higher permeability and selectivity for applications where such improvements matter; and (iii) more emphasis on fundamental structure/property/processing relations. There is a pressing need for membranes with improved selectivity, rather than membranes with improved permeability, especially for water purification. Modeling at all length scales is needed to develop a coherent molecular understanding of membrane properties, provide insight for future materials design, and clarify the fundamental basis for trade-off behavior. Basic molecular-level understanding of thermodynamic and diffusion properties of water and ions in charged membranes for desalination and energy applications such as fuel cells is largely incomplete. Fundamental understanding of membrane structure optimization to control transport of minor species (e.g., trace-organic contaminants in desalination membranes, neutral compounds in charged membranes, and heavy hydrocarbons in membranes for natural gas separation) is needed. Laboratory evaluation of membranes is often conducted with highly idealized mixtures, so separation performance in real applications with complex mixtures is poorly understood. Lack of systematic understanding of methodologies to scale promising membranes from the few square centimeters needed for laboratory studies to the thousands of square meters needed for large applications stymies membrane deployment. Nevertheless, opportunities for membranes in both existing and emerging applications, together with an expanding set of membrane materials, hold great promise for membranes to effectively address separations needs. ■

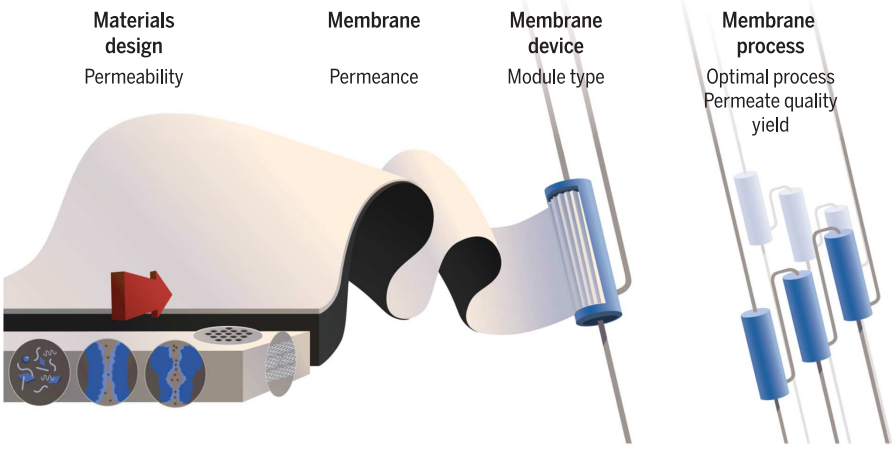

From intrinsic permeability/selectivity trade-off to practical performance in membranes. Polymer membranes for liquid and gas separation applications obey a permeability/selectivity trade-off—highly permeable membranes have low selectivity and vice versa—largely due to broad distributions of free-volume elements (or pores in porous membranes) and nonspecific interactions between small solutes and polymers. We highlight materials approaches to overcome this trade-off, including the development of inorganic, isoporous, mixed matrix, and aquaporin membranes. Further, materials must be processed into thin, typically supported membranes, fashioned into high surface/volume ratio modules, and used in optimized processes. Thus, factors that govern the practical feasibility of membranes, such as mechanical strength, module design, and operating conditions, are also discussed.

Author affiliations are available in the full article online.
*Corresponding author. Email: freeman@che.utexas.edu
Cite this article as H. B. Park *et al.*, *Science* **356**, eaab0530 (2017). DOI: 10.1126/science.aab0530

REVIEW

MEMBRANES

Maximizing the right stuff: The trade-off between membrane permeability and selectivity

Ho Bum Park,[1] Jovan Kamcev,[2] Lloyd M. Robeson,[3] Menachem Elimelech,[4] Benny D. Freeman[2]*

Increasing demands for energy-efficient separations in applications ranging from water purification to petroleum refining, chemicals production, and carbon capture have stimulated a vigorous search for novel, high-performance separation membranes. Synthetic membranes suffer a ubiquitous, pernicious trade-off: highly permeable membranes lack selectivity and vice versa. However, materials with both high permeability and high selectivity are beginning to emerge. For example, design features from biological membranes have been applied to break the permeability-selectivity trade-off. We review the basis for the permeability-selectivity trade-off, state-of-the-art approaches to membrane materials design to overcome the trade-off, and factors other than permeability and selectivity that govern membrane performance and, in turn, influence membrane design.

Synthetic membranes, based largely on polymers, are widely used in gas separations (e.g., air dehydration; O_2/N_2 separation; hydrogen purification; and CO_2, H_2S, and higher hydrocarbon removal from natural gas), water purification (e.g., desalination, ultrapure water production, drinking water treatment, and municipal and industrial wastewater treatment and reuse) (*1*–*3*), bioprocessing (e.g., sterile filtration, protein concentration, and buffer exchange) (*4*, *5*), medical applications (e.g., dialysis, blood oxygenation, and drug delivery) (*6*), food processing (e.g., beer and wine clarification and demineralization of whey, juices, and sugar) (*7*, *8*), chemicals production (e.g., chlor-alkali process to produce chlorine and sodium hydroxide) (*8*), batteries (*9*), and fuel cells (*10*, *11*). Potential applications include energy generation (*12*, *13*); energy storage (*14*); environmental applications such as carbon capture (*15*) and selective removal of ions (e.g., nitrates and phosphates) contributing to surface water eutrophication (*16*); organic solvent recovery (*17*); pharmaceutical purification (*18*); catalyst recovery (*18*); and membrane crystallization (*19*), distillation (*3*, *19*), and emulsification (*20*). In many applications, membranes are favored over other processes due to advantages in energy efficiency, simplicity, manufacturing scalability, and small footprint (*1*–*3*). However, all synthetic membranes are subject to a trade-off between permeability and selectivity, as well as practical challenges such as fouling, degradation, and material failure that limit their use.

[1]Department of Energy Engineering, Hanyang University, Seoul 04763, Republic of Korea. [2]Department of Chemical Engineering, Texas Materials Institute, Center for Research in Water Resources, and Center for Energy and Environmental Research, The University of Texas at Austin, 10100 Burnet Road, Building 133 (CEER), Austin, TX 78758, USA. [3]Department of Materials Science and Engineering, Lehigh University, 1801 Mill Creek Road, Macungie, PA 18062, USA. [4]Department of Chemical and Environmental Engineering, Yale University, New Haven, CT 06520-8286, USA.
*Corresponding author. Email: freeman@che.utexas.edu

Origin of the permeability-selectivity trade-off

The commercialization of polymeric membranes for gas separations in the late 1970s catalyzed a sustained search for materials with better separation properties. As the database of gas permeation properties on various materials expanded, researchers discovered a trade-off between gas permeability, P_i (see Box 1 for definition), and selectivity, $\alpha_{i,j} = P_i/P_j$, where i represents the more permeable gas of the i, j gas pair (e.g., i = O_2 and j = N_2 in air separation) (*21*). During the 1980s, permeability data on six common gases (He, H_2, O_2, N_2, CO_2, and CH_4) were compiled, and the trade-off relationship between permeability and selectivity was analyzed. Polymers having the highest selectivity at a given permeability lay near or on a line, called the upper bound, obeying the following relation (*21*)

$$\alpha_{i,j} = \beta_{i,j} P_i^{-\lambda_{i,j}} \quad (1)$$

where $\lambda_{i,j}$ and $\beta_{i,j}$ are parameters depending on the gas pair. An example for air separation (i.e., O_2/N_2 separation) is shown in Fig. 1A. More permeable polymers tend to have lower selectivity, and vice versa. This study (*21*) became the standard against which permeability and selectivity values for new and improved membrane materials were measured.

A theoretical model of the permeability/selectivity trade-off (*22*) revealed that the slope, $\lambda_{i,j}$, depends on the ratio of gas molecule diameters, $\lambda_{i,j} = (d_j/d_i)^2 - 1$, where d_j and d_i are the kinetic diameters of the larger and smaller gases, respectively, and upper-bound behavior was found for all gas pairs reported. The front factor, $\beta_{i,j}$, depends on gas solubility, $\lambda_{i,j}$, and an adjustable constant, f, related to the average distance between polymer chains and chain stiffness. This model was based on five hypotheses: (i) gas permeation occurs via the solution-diffusion mechanism (see Box 1); (ii) gas diffusion is an activated process, described by an Arrhenius equation; (iii) the activation energy of diffusion, E_D, of a gas molecule depends on the square of its effective size; (iv) a universal linear free-energy relation exists between E_D and the front factor in the Arrhenius equation; and (v) gas solubility depends on gas molecule condensability, as expressed, for example, by the Lennard-Jones well depth of the gas molecule.

The 1991 upper-bound results (*21*) were revisited in 2008 with a much larger database and notable advances in the search for more permeable and selective polymers (*23*). In most cases, only modest shifts in the upper bound were observed despite many studies between 1991 and 2008 aimed at preparing materials to exceed the upper bound. This point is illustrated in Fig. 1A where the 1991 and 2008 upper bounds are superimposed. Notably, and in agreement with the upper-bound model (*22*), the slopes, $\lambda_{i,j}$, of the upper bound did not change, but the position of the upper bound, $\beta_{i,j}$, moved as shown in Fig. 1A for all gas pairs considered.

The most significant changes in $\beta_{i,j}$ values were with He-based gas pairs (specifically He/H_2), where glassy perfluorinated polymers came to dominate the upper bound (*23*). Perfluoropolymers exhibit unique gas solubility characteristics relative to aromatic and other hydrocarbon polymers, for reasons still unresolved at a fundamental level (*24*, *25*). These solubility characteristics account for the presence of perfluoropolymers at the upper bound for some gas pairs.

For other gas pairs, $\beta_{i,j}$ values changed due to introduction of new materials. Two classes of polymers—PIMs (polymers of intrinsic microporosity, e.g., polybenzodioxanes) (*26*) and TRs (thermally rearranged polymers, e.g., polybenzoxazoles) (*27*)—gave exceptional performance. For CO_2/CH_4, several TR polymers significantly exceeded the upper bound. The bases for their unusually high permeability/selectivity combinations are (i) high gas solubility, an inherent characteristic of high free-volume glassy polymers such as PIMs and TR polymers; (ii) high gas diffusion coefficients, which are also a consequence of high free volume; and (iii) for several gas pairs (e.g., O_2/N_2 and CO_2/CH_4), unusually high gas diffusion selectivity, suggesting size and size distribution of free-volume elements in a range particularly suitable for separating these gas molecules based on sub-Angstrom differences in effective gas molecule size (*28*).

A comparison of rubbery versus glassy (i.e., flexible versus rigid) polymers (*29*) revealed that gas solubilities are uniformly higher in glassy

than rubbery polymers when compared at equivalent permeabilities, due to additional sorption of gas into the nonequilibrium excess volume inherently present in glassy polymers (i.e., dual-mode sorption) (*30*). Thus, glassy polymers dominate the upper bound mainly due to higher gas solubility than rubbery polymers (*29*). When compared at equivalent free-volume levels, rubbery and glassy polymers have very similar diffusion selectivities (*29*). That is, for most polymers, diffusion selectivity differences between glassy and rubbery polymers only modestly favor glassy polymers, in contrast to generalizations previously reported and accepted in the literature.

Various approaches to exceed the upper bound have been explored, including surface modification (*31*, *32*), facilitated transport (*33*), phase-separated polymer blends (*34*), and mixed-matrix membranes (MMMs) (*35*). Although the upper-bound concept as originally formulated only applies to homogeneous polymer membranes, comparing permeability and selectivity data on upper-bound plots remains a popular way to gauge membrane material performance. In addition to the upper-bound pairs possible from the six gases noted above, upper-bound relationships have been reported for other important gas pairs, such as propylene/propane (*36*), ethylene/ethane (*37*), and N_2/NF_3 (*38*).

Other examples of such trade-off behavior have emerged in virtually all synthetic polymer membranes, including desalination membranes (*39*) (Fig. 1B), forward osmosis membranes (*40*–*42*), porous ultrafiltration (UF) membranes (*43*) (Fig. 1C), polymer electrolyte membranes for fuel cells (*44*) (Fig. 1D), pervaporation membranes (*45*), and ion-exchange membranes (*46*). The fundamental physics of small-molecule transport through dense, nonporous polymers (e.g., for gas separation and water/salt separation (*47*)) are different from those of proteins through porous UF membranes and ion transport through charged polymers in electrically driven separations (*3*, *5*, *8*, *43*). Nevertheless, upper-bound behavior is observed in all cases, suggesting the generality of this phenomenon in both dense and porous membranes. Additionally, materials used to form either porous or dense membranes do not necessarily have to be polymeric for the resulting membranes to exhibit permeability-selectivity trade-offs (*48*).

Common features of the dense polymer membranes mentioned above are a broad distribution of free-volume element sizes, as shown in Fig. 2, A and B, and relatively nonspecific interactions governing solubility of small molecules in polymers (*3*, *27*, *30*). Changing a polymer structure to give more rapid permeation often enhances permeability of larger species more than smaller species, resulting in increased permeability but decreased selectivity. This pattern has been ascribed to a lack of ability to increase free-volume element size while simultaneously narrowing free-volume element size distribution (*27*). Membranes with very narrow pore size distributions are "isoporous" membranes (i.e., those with uniform pore sizes), as shown in Fig. 2, C and D. Such

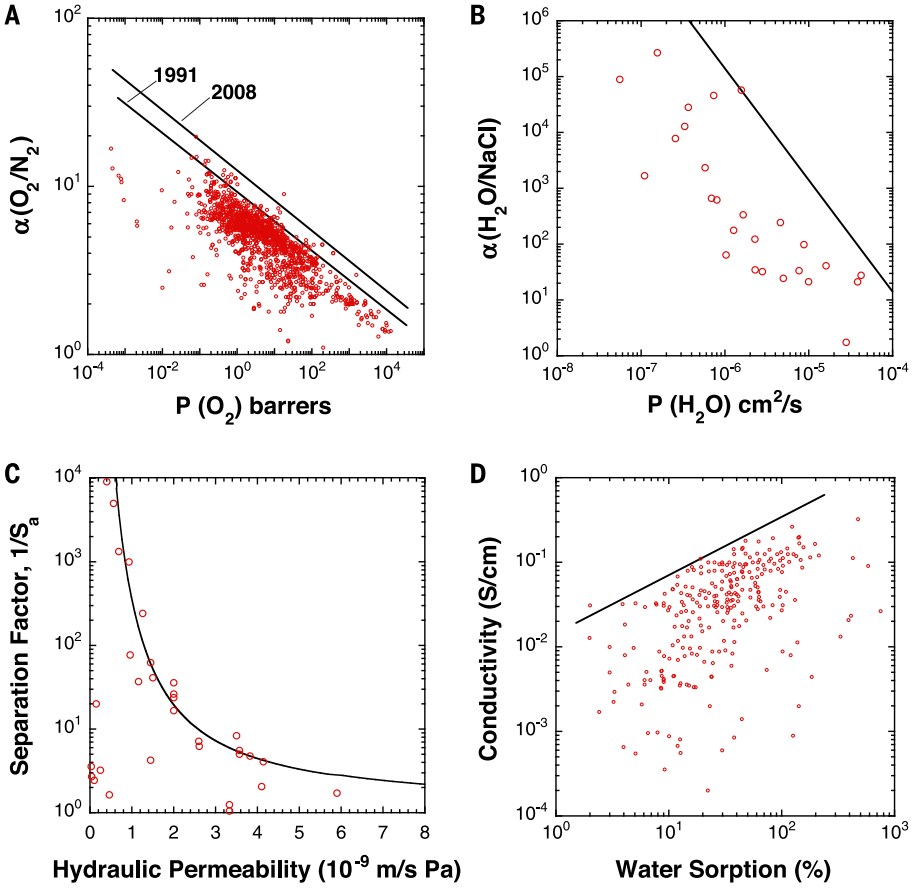

Fig. 1. Upper-bound relations in polymer membranes. (**A**) O_2/N_2 separation (*23*); (**B**) water/salt separation (*39*); (**C**) protein/water separation in porous ultrafiltration membranes [$1/S_a$ is the separation factor of bovine serum albumin (BSA) from water and other small solutes (e.g., salts and sugars)], and hydraulic permeability is the rate of transport through the membrane of water and any solutes not retained by the membrane (*43*); and (**D**) polymer electrolyte membranes, where ionic conductivity for membranes at a given level of water uptake (i.e., water sorption) is apparently limited by an upper-bound type relationship (*44*).

Box 1. Solution-diffusion transport mechanism in nonporous polymers. Gas permeability is defined as $P_i = N_i L/\Delta p$, where N_i is the steady-state flux of gas i through the membrane, L is membrane thickness, and Δp is the transmembrane pressure difference (or partial pressure difference, in the case of gas mixtures). The three-step solution-diffusion mechanism is the accepted framework for small-molecule transport in nonporous polymers (*120*). A penetrant molecule (i) dissolves into the upstream (i.e., high concentration) side of a membrane, (ii) diffuses through the membrane, and (iii) desorbs from the downstream (i.e., low concentration) side of a membrane. The second step is the rate-limiting step in all current membranes, and the rate-limiting step in gas diffusion through polymers is the local segmental dynamics of the polymer chains, which open transient gaps (i.e., free-volume elements) through which gas diffusion occurs. In this framework, permeability is written as $P_i = S_i D_i$, where S_i and D_i are the penetrant solubility and diffusivity in the polymer, respectively, and $\alpha_{i,j} = (S_i/S_j) \times (D_i/D_j)$, where S_i/S_j and D_i/D_j are the solubility and diffusivity selectivities, respectively. The same mechanism applies to water and salt transport in RO membranes and other membrane processes involving nonporous materials (*120*). The gas permeability unit is the barrer, where 1 barrer $= 10^{-10} \frac{\text{cm}^3(\text{STP})\ \text{cm}}{\text{cm}^2\ \text{s cmHg}}$. Gas flux is often normalized by pressure to give permeance, $P_i/L = N_i/\Delta p$, which is reported in gas permeation units (GPU), where 1 GPU $= 10^{-6} \frac{\text{cm}^3(\text{STP})}{\text{cm}^2\ \text{s cmHg}}$. In RO desalination membranes, the equivalent expression for water flux, N_w, is $N_w = A(\Delta p - \Delta\pi)$, where A (i.e., permeance) contains the membrane permeability to thickness ratio, Δp is the applied hydrostatic pressure, and $\Delta\pi$ is the osmotic pressure difference across the membrane, generated by the difference in salt concentration on either side of the membrane (*121*).

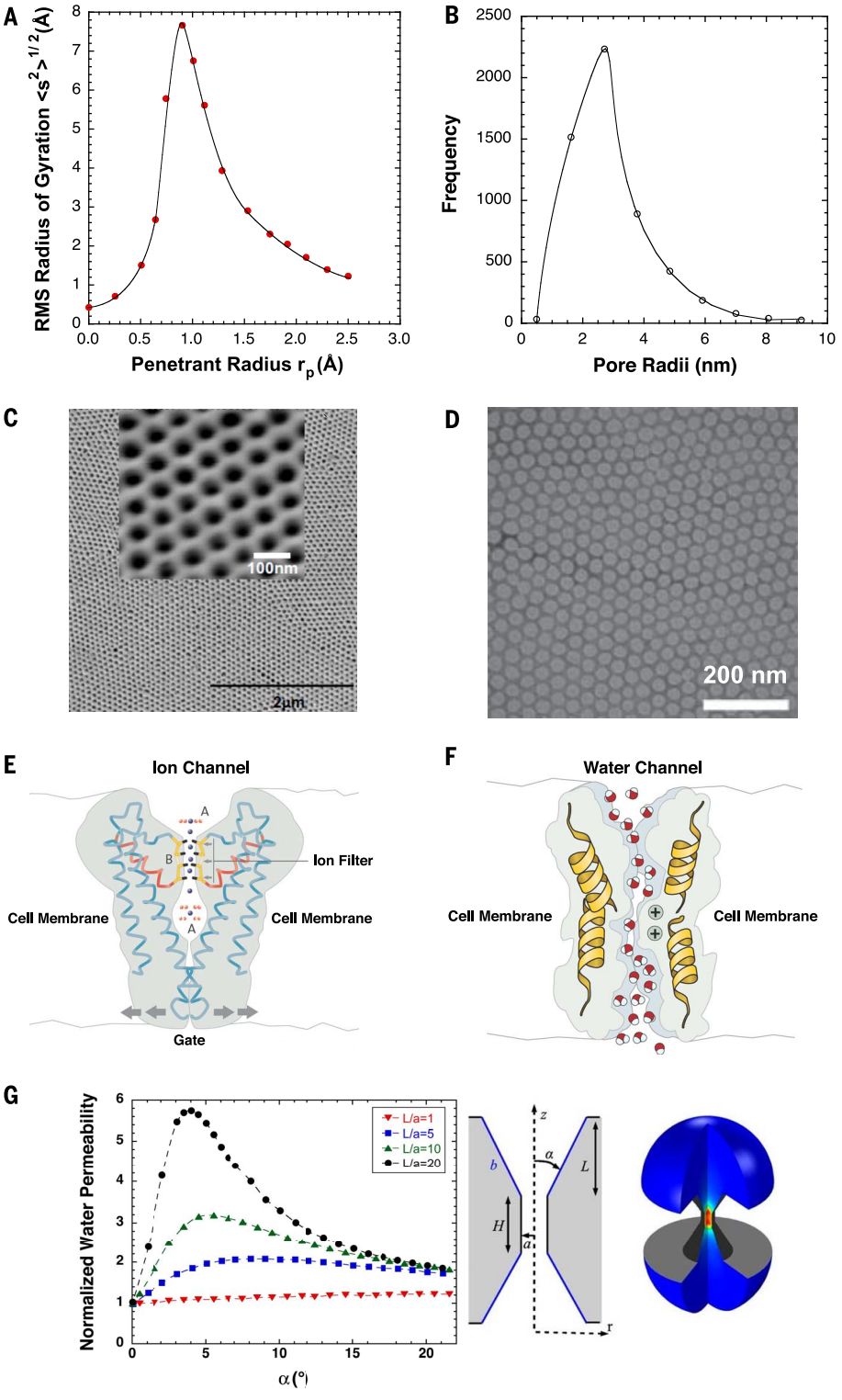

Fig. 2. Evolution of cavity (or pore) size distributions in membranes. Cavity (or pore) size distributions in separation membranes, ranging from (**A**) broad cavity-size distributions in dense polymers, such as those used in gas separations (*113*) and (**B**) water purification (e.g., porous ultrafiltration membranes) (*114*) to narrow pore size distributions in (**C**) isoporous UF membranes formed via self-assembly of block copolymers (~34-nm pore diameter) (*52*), (**D**) graphene nanomesh having ~30-nm pores prepared via block copolymer lithography (*115*), (**E**) potassium ion channel (*116*), (**F**) aquaporin (*93*), and (**G**) the effect of hourglass pore design parameters (pore opening angle, α, and aspect ratio, *L*/a) on water permeability (*117*).

membranes can have both high permeability and high selectivity because the isoporous geometry contributes to membranes with no tortuosity (high permeability) and precise, uniform pore size (high selectivity). However, practical development of these membranes is in its infancy.

Design approaches for improved permeability and selectivity

Biological membranes, such as potassium ion channels and aquaporins (Fig. 2, E and F), have extremely high selectivity-permeability combinations, which has stimulated recent efforts aimed at (i) direct incorporation of such structures into membranes (*49*), (ii) theoretical studies aimed at understanding optimal structures (Fig. 2G) that might yield high permeability and selectivity, or (iii) synthetic membrane structures that mimic or are inspired by one or more elements of biological membranes. So far, incorporation of, for example, aquaporins into membranes has been done via assimilation of aquaporins into vesicles and integration of the resulting vesicles into membranes, but there are no successful, reproducible studies demonstrating that this strategy can produce highly selective membranes (*48*). Thus, much remains uncertain about their ability to be processed into the large-scale, defect-free structures required for practical applications or whether they can maintain adequate transport and selectivity properties upon exposure to complex, real-world feed mixtures for extended periods of time. We return to these points below.

Certain structural changes in polymers used for gas separation, such as thermal rearrangement, narrow an otherwise broad free-volume element size distribution. This contributes to higher permeability-selectivity combinations, but such materials still have a wide distribution of free-volume elements relative to biological membranes (*27*). Block copolymers innately self-assemble into well-defined structures with regular periodicity. This phenomenon has been harnessed to prepare ~15-nm-diameter isoporous membranes with complete rejection of virus particles and high water flux (*50*). This concept was extended to prepare isoporous UF membranes via nonsolvent-induced phase inversion (NIPS), an industrial process used to produce many current membranes, providing a potential route to large-scale production of such structures (*51*). Optimization of this process led to water permeances of 3200 L $m^{-2}h^{-1}bar^{-1}$, an order of magnitude higher than conventional NIPS membranes of the same average pore size, coupled with a selectivity of 87 for separating bovine serum albumin (MW = 67 kDa, diameter ~6.8 nm) from globulin-γ (MW = 150 kDa, diameter ~14 nm), proteins too close in size to be separated by conventional UF membranes (*52*). The high water permeance in such isoporous membranes was due to higher porosity and lower tortuosity at similar pore size relative to conventional UF membranes. Typically, such self-assembled structures can be used to make isoporous membranes with pore sizes ranging from 3 to 20 nm, in the range of UF membranes. Using mixtures of different block copolymers,

the pore size was reduced to ~1.5 nm, while still maintaining high water flux (53), yielding nanofiltration (NF) membranes, thereby potentially opening a large set of practically important separations (e.g., dye removal from textile wastewater). The detailed formation mechanism of such membranes is still under debate (54). Block copolymers, such as those used to prepare the original isoporous membranes, are expensive relative to traditional polymers used in water-purification membranes. If isoporous membrane were made entirely of such block copolymers, cost would likely be a considerable roadblock for such materials, restricting their use to high-value, low-volume separations (e.g., biomedical applications) rather than large-scale drinking or wastewater purification applications.

Inorganic materials offer efficient ways to tailor pore sizes and shapes and achieve narrow pore size distributions, potentially leading to high permeability and/or high selectivity. For example, metal-organic frameworks (MOFs) have been studied for gas separation and other related applications (55). MOFs are synthesized by connecting inorganic and organic units via covalent bonds to form permanently porous crystalline structures. Numerous MOFs with various well-defined pore sizes and channels have been reported (56). Due to their high porosity (~50% of the crystal volume); high surface area (~10,000 m^2g^{-1}), which exceeds traditional inorganic materials (e.g., zeolites and carbon molecular sieves); and extensive ability to chemically tailor MOFs, they have been widely studied as membrane materials. Crystalline MOF membranes on porous substrates have been explored, particularly for gas separation applications. Like zeolite membranes, continuous MOF membranes are prepared primarily by in situ and seeded-secondary growth methods. More recently, zeolitic imidazole frameworks (ZIFs), a subclass of MOFs, have been of interest for gas separations, mainly because their pore size is similar to the size of small gas molecules and they can exhibit high chemical and thermal stability (57, 58).

Although continuous, self-supporting thin films of MOFs would be preferred for membrane applications, they are not mechanically robust enough to form large surface area membranes. Consequently, they are fabricated on mechanically stable porous supports (58). Additionally, such crystalline materials in the thin-film state contain intrinsic or extrinsic defects (e.g., grain boundaries) between single crystalline domains, leading to nonselective flow (59). Many studies focus on minimizing such defects to achieve high selectivity and reducing the thickness of the active layer to achieve high permeance. For example, Nair and colleagues. coated ZIF-8 onto polymeric hollow fibers using two-solvent interfacial synthesis (58). They used highly gas-permeable, porous poly(amide-imide) hollow fibers as a support and prepared a continuous ZIF-8 membrane on the lumen surface of the hollow fibers via interfacial microfluidic membrane processing. These membranes showed clear molecular sieving properties—high H_2 permeance [3000 gas permeation units (GPU)], high H_2/C_3H_8 selectivity (130 at 120°C), and a strong temperature dependence of H_2 permeance, implying activated molecular transport through the ZIF-8 pores. When defects were sealed with poly(dimethylsiloxane), the H_2/C_3H_8 selectivity increased to 370, but H_2 permeance decreased to 750 GPU. ZIF-8 has an effective aperture (i.e., pore) size of ~4.0 Å, so it may be of interest for propylene/propane separation, a large-scale, highly energy-intensive separation (36). More recently, Kwon *et al.* reported heteroepitaxially grown ZIF membranes consisting of two different ZIF layers (60). Submicrometer-thick ZIF-67 membranes were heteroepitaxially grown from ZIF-8 seed layers on alumina supports. Addition of a ZIF-8 overlayer (~300 nm) on a ZIF-67 membrane led to very high propylene/propane separation factor (~200) with high propylene permeability, well above the upper bound for both polymer and carbon membranes (36). However, since alumina is a brittle ceramic, this approach does not solve the basic mechanical property challenge facing such materials, rendering scale-up of these membranes unlikely.

Graphene and other two-dimensional (2D) atomically thin materials (e.g., graphdiyne, graphyne, hBN, and MoS_2, 2D polymers based on polyphenylene, porphyrin, and cyclohexa-m-phenylene, etc.) have attracted attention because of the minimum possible thickness, high mechanical strength, chemical stability, and ability to create selective nanoscale pores in their rigid 2D lattices (61). Two distinct strategies to use such materials (e.g., graphene) for membranes have been reported: (i) creating nanopores (or defects) in the basal plane (62) or (ii) tailoring the 2D nanochannels inherently present between stacked 2D sheets (e.g., graphene oxide or reduced graphene oxide) (63). Simulations suggest that monolayer porous graphene could be highly permeable and selective, with higher separation performance than polymer membranes. Gas separation and water/ion separation properties have been measured using such porous graphene membranes (62, 64). Precisely tuning the nanochannels between stacked 2D graphene sheets, or controlling the pore size and achieving high porosity with large-area graphene membranes, pose considerable technological challenges due to defect control in raw graphene monolayers. Therefore, such materials cannot be used for industrial, large-area membranes without major breakthroughs in large-scale, reproducible manufacturing.

As an example of the properties of such materials, Surwade *et al.* created small nanopores (~1 nm) via oxygen plasma irradiation at a density of ~10^{12} cm^{-2} in monolayer graphene membranes placed on a microscale aperture. The resulting membranes exhibited high water permeability (64). In one sample, the driving force normalized water flux (i.e., permeance) was 250 L $m^{-2}h^{-1}bar^{-1}$, whereas a state-of-the-art reverse osmosis (RO) membrane would have a permeance of about 2.3 L $m^{-2}h^{-1}bar^{-1}$ (65–68). However, this perforated graphene membrane had poor salt/water selectivity, ranging from about 5 to 200 (the wide range presumably due to sample-to-sample variability). For comparison, a state-of-the-art RO membrane requires a salt/water selectivity of 16,000 to meet water purity requirements, and aquaporins have essentially infinite selectivity and a permeance of 1.6 × 10^6 L $m^{-2}h^{-1}bar^{-1}$ per aquaporin (68).

Graphene oxide (GO) has a high density of oxygen-containing functional groups (e.g., hydroxyl, epoxy, and carboxyl) and some vacancy defects in the 2D carbon lattice. GO can be prepared inexpensively on a large scale by oxidation and exfoliation of graphite. GO sheets can be readily dispersed in water or organic solvents, providing facile means for membrane fabrication via well-developed membrane-coating technology using GO dispersions (69, 70). Differing from nanoporous graphene, adjustable 2D nanochannels between adjacent GO sheets can be used for selective molecular transport. GO membranes can have high water-transport rates (71), because the oxidized domains act as spacers to separate adjacent GO sheets and facilitate water molecule intercalation, and the pristine graphitic domains in GO sheets create a network of capillaries allowing almost frictionless flow of water, similar to water transport through carbon nanotubes (72). In addition, GO membranes can display sieving properties in aqueous solutions (69), blocking all solutes with hydrated radii larger than 0.45 nm, which is inadequate for desalination applications, given that, for example, a hydrated sodium ion is smaller than this.

GO membranes have also been explored for gas separations. Li *et al.* (73) fabricated ultrathin GO membranes (e.g., ~1.8 nm thick) that exhibited high H_2/CO_2 and H_2/N_2 selectivity. Kim *et al.* (63) demonstrated that hydrated thin GO membranes can be used as CO_2-selective membranes because permeance of all gases, except CO_2, decreased as feed humidity increased. Condensed water molecules in the pores, or between GO sheets, hindered transport of relatively noncondensable small molecules such as N_2. As with graphene and other 2D atomically thin materials discussed before, fabrication of defect-free, large-scale GO membranes for liquid or gas separation is extremely challenging, due to their poor mechanical properties, which markedly limits the practicality of such membranes.

On the laboratory scale, a 10 cm^2 (10^{-3} m^2) membrane sample is often sufficient to generate initial characterization data. However, industrial production of membranes for large-scale applications can require 1000 to 100,000 m^2 of membranes, all of which must be prepared with defect densities, for gas separations, below about 1 cm^2 of defects for every 10^5 cm^2 of membrane surface area (74, 75). Such a 10^6 to 10^8 scale-up in the size of defect-free membranes is often a major stumbling block for introduction of new materials as membranes and is exacerbated if the new materials cannot be readily transformed into thin, defect-free membranes using conventional membrane-formation methods (3).

One popular approach to address difficulties in preparing large-surface-area, defect-free, ultrathin membranes of promising nanomaterials (e.g., carbon nanotubes, graphene, zeolites, and MOFs) is the use of mixed-matrix membranes (MMMs).

MMMs commonly consist of a dispersed nanomaterial phase and a continuous polymer matrix, hoping to marry the high intrinsic permeability and separation properties of advanced nanomaterials with the robust processing and mechanical properties of polymers (Fig. 3). Most studies involving MMMs have focused on gas separation membranes (*76*), in which molecular sieving particles such as zeolites, carbons, and MOFs have been incorporated into a polymer matrix to alter their performance. More recently, nanotubes and nanosheets have been considered as the dispersed phase (*77*, *78*). Koros and colleagues theoretically analyzed the potential of MMMs, predicting gas separation performance beyond Robeson's upper bound (particularly for O_2/N_2 separation) (*35*). However, most experimental results fall below the theoretical maximum because of unfavorably large interfacial gaps between the dispersed nanomaterials and polymer matrix and relatively limited dispersed phase loading due to particle agglomeration (*79*). As such, much of the effort to enhance separation performance in MMMs focuses on reducing the incompatibility between inorganic materials and organic polymers, while achieving homogeneous dispersions at high loading levels (*80*, *81*). However, despite well over a decade of sustained efforts to develop large-scale, practical MMMs, there are no commercial examples of such membranes. Uniformly dispersing nanomaterials in thin polymer selective layers (e.g., <100 nm thick) via continuous processes (e.g., hollow fiber spinning) to make reproducible, large-surface-area membranes, without introducing selectivity-destroying defects while maintaining sufficient mechanical properties to permit manufacturing and use of the resulting membranes, has proven an arduous undertaking due to the large number of processing variables affecting the final material structure.

In principle, in the absence of significant interfacial gaps and with homogeneous dispersion, inclusion of inorganic materials can improve membrane performance by increasing selectivity, permeability, or both. Interfacial compatibility, interaction energy between nanomaterials and polymers, type of nanomaterial (e.g., zeolites, silica, carbon molecular sieves, activated carbon, MOFs, carbon nanotubes, metal oxides, mesoporous materials, nonporous materials, and nanosheets), nanomaterial concentration, orientation of anisotropic nanomaterials, and permeation properties of the polymer continuous phase all influence membrane performance (*77*, *82*, *83*). Scalable processing of MMMs is less difficult than processing membranes made solely from novel nanomaterials (e.g., MOFs and carbon nanotubes) but can be much more difficult than processing polymers alone. Successfully including such nanomaterials into thin, selective polymer layers less than 100 nm thick requires small filler size. Bachman *et al.* reported MOF nanocrystals dispersed in a polyimide membrane for olefin/paraffin separation (*55*). Small MOF nanocrystals (17 to 18 nm), having high external surface area, led to a greater fraction of polymer at the polymer/MOF interface, thereby reducing the number of nonselective pathways for gas transport, resulting in high ethylene/ethane separation performance with increasing MOF content (*55*). Incorporation of larger MOFs (i.e., 100 to 200 nm) did not show performance improvement relative to that of membranes containing smaller MOF nanocrystals.

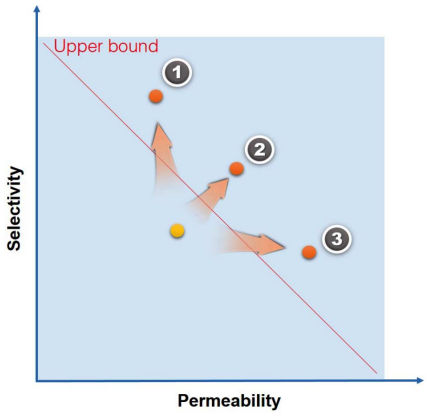

Fig. 3. In designing mixed-matrix membranes to overcome the upper bound, compatibility between filler and polymer, filler particle size and shape, and homogeneous filler distribution are important factors. (**Case 1**) Molecular sieving fillers (e.g., CMS and zeolites) often lead to selectivity increases and permeability decreases (*35*). (**Case 2**) Molecular sieving fillers with nano size or nanosheet shapes (e.g., MOFs nanocrystals or 2D nanosheets) can improve both permeability and selectivity (*55*). (**Case 3**) Fillers with interfacial voids, even when homogeneously dispersed, can result in increased permeability and decreased selectivity (*55*).

In addition to the factors discussed above, filler shape and orientation are important. Anisotropically shaped (e.g., sheetlike) inorganic materials may be better than isotropically shaped materials for mixed-matrix membranes, because MMMs containing nanoscopically small, thin nanosheets can allow high separation performance at much lower loading than that required for isotropic fillers. For example, 2D nanomaterials [i.e., those with one dimension on the nanoscale (e.g., MOF nanosheets and graphene oxide)], rather than 0D [all three dimensions on the nanoscale (e.g., carbon molecular sieves, silica, and MOF crystals)] or 1D [two dimensions on nanoscale (e.g., carbon nanotubes and aluminosilicate nanotubes)] nanomaterials, may be preferred because they can be incorporated into ultrathin membranes such as the selective skin layers of thin-film composite or hollow fiber membranes. MOF nanosheets exhibiting high gas permeance and high gas selectivity (e.g., H_2/CO_2 separation) have been developed (*84*). When such MOF nanosheets are incorporated into a polymer matrix, the resulting MMMs can improve gas separation performance by eliminating nonselective permeation pathways as compared with isotropic MOFs. Rodenas *et al.* compared the CO_2/CH_4 selectivity with MMMs, including a bulky-type MOF, nanosized MOF, and MOF nanosheets, based on the same MOF material (*85*). Only MOF nanosheets in the MMM showed improved selectivity and no significant permeability loss relative to the neat polymer membrane. Similar effects can be observed in other nanosheet-incorporated MMMs. When GO nanosheets are incorporated into polyether-based copolymer membranes for CO_2 separation, CO_2/N_2 selectivity increased significantly compared with the pristine polymer membrane with no permeability penalty, even at low loadings (e.g., below 0.1 weight %) (*86*).

Comparison of transport characteristics of synthetic and biological membranes

Unlike synthetic membranes, biological membranes exhibit both high permeability and high selectivity. For example, the potassium ion channel in cell membranes is thousands of times more permeable to potassium than sodium ions, despite the smaller ionic (i.e., crystallographic) size of sodium, and exhibits permeation rates (~10^8 ions/s) approaching the diffusion limit (*87*). Polymer membranes often exhibit little selectivity for ions of like valence and transport such ions orders of magnitude more slowly. For example, McGrath *et al.* reported NaCl and KCl permeability coefficients of 3.8×10^{-8} cm^2 s^{-1} and 4.4×10^{-8} cm^2 s^{-1}, respectively, in a di-sulfonated poly(arylene ether sulfone) membrane (*88*). KCl permeation was more rapid than NaCl permeation by a factor of ~1.2, whereas in potassium ion channels, K^+ is thousands of times more permeable than Na^+ (*87*, *89*).

Rates of K^+ transport in ion channels may be up to 10^8 ions/s (*87*). The diameter of the selectivity filter is approximately 0.3 nm, so the area available for ion transport is 0.071 nm^2. Thus, the K^+ flux through the selectivity filter is 0.235 mol/(cm^2 s). A typical extracellular K^+ concentration is 4 mM, and a typical intracellular K^+ concentration is 155 mM (*90*). The length of the selectivity filter is 1.2 nm (*87*). On this basis, the permeability coefficient of K^+, P_{K^+}, is estimated as follows (*39*, *91*): $P_{K^+} = J_{K^+}L/\Delta C_{K^+}$, where J_{K^+} is the flux of K^+, L is the length of the selectivity filter, and ΔC_{K^+} is the K^+ concentration difference between the extracellular and intracellular compartments. Thus, the K^+ permeability of an ion channel, P_{K^+}, is 1.9×10^{-4} cm^2 s^{-1}, ~4 orders of magnitude faster than that reported by McGrath *et al.*

As a further comparison, the Na^+ permeability of a Nafion synthetic ion exchange membrane was calculated using data reported by Pintauro and Bennlon (*92*). The Na^+ concentration in Nafion equilibrated with a 1 M NaCl solution was 1.21 mol L^{-1} (swollen membrane). The diffusion coefficient of Na^+ in the membrane at the same conditions was 2.62×10^{-6} cm^2 s^{-1}. The Na^+ permeability, P_{Na^+}, was calculated using the solution-diffusion model (*91*): $P_{Na^+} = C^m_{Na^+} D_{Na^+} / C^s_{Na^+}$, where $C^m_{Na^+}$ is the Na^+ concentration in the membrane, $C^s_{Na^+}$ is the Na^+ concentration in the solution contiguous to the membrane (1 M), and D_{Na^+}

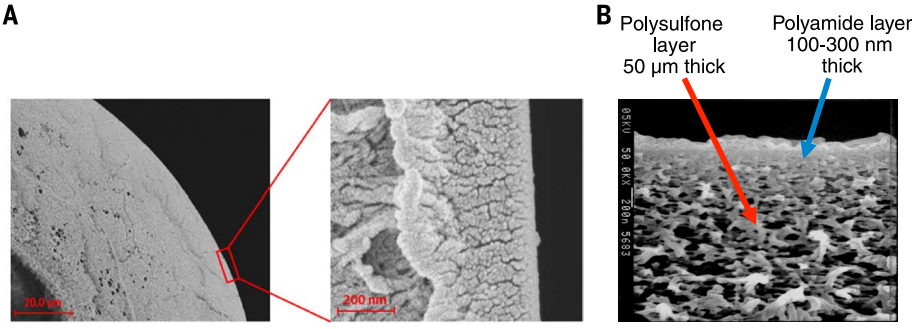

Fig. 4. Morphology of state-of-the-art membranes. Examples of (**A**) hollow fiber gas separation membrane (*118*) and (**B**) flat sheet RO membrane (*91*).

is the sodium diffusion coefficient in the membrane. Thus, the Na^+ permeability in Nafion was 3.1×10^{-6} cm^2 s^{-1}, nearly two orders of magnitude lower than that of the potassium ion channel, demonstrating the high permeability of ion channels relative to synthetic membranes.

In aquaporins, water can transport as fast as ~3×10^9 molecules/s through the water channel, whereas H_3O^+ and small neutral solutes are almost completely excluded (*48*, *93*–*95*). Such transport properties are simply unattainable with current synthetic membranes (*68*). These combinations of high selectivity and permeation are ascribed to several common structural features in both aquaporins and potassium ion channels: (i) uniform pore sizes of just the right size to accommodate the desired ion or water molecule; (ii) hourglass-shaped pores, with a very short selectivity filter [i.e., 12 Å long in the potassium channel (*87*) and ~20 Å in AQP1 aquaporin (*93*)], flanked by wider regions (i.e., vestibules) to accommodate rapid ion or water transport to and from the selectivity filter; and (iii) exquisitely tuned molecular interactions to energetically and entropically facilitate partitioning of desired species into the channel (*87*, *93*).

Direct incorporation of bacterial water channel proteins [aquaporin Z (AQP)] into synthetic membranes can lead to improved combinations of water transport and salt rejection in desalination membranes. In 2007, Kumar *et al.* reported successful insertion of AQP proteins into synthetic triblock copolymer vesicles to form spherical cavities (~117-nm radius) with AQP units spanning the vesicle wall (*96*). The rate of water transport through the vesicle walls increased 5 to 10 times upon introduction of AQP. To create a functional membrane, AQP-containing vesicles were ruptured onto a porous support membrane to form a planar bilayer, which acted as the selective barrier of the membrane (*97*). Such membranes generally exhibited low salt rejection due to unavoidable defects. Another approach is to incorporate AQP-containing vesicles into the aqueous diamine solution commonly used to prepare NF and RO membranes by interfacial polymerization (*98*). However, separation performance of membranes prepared by this simple approach is mostly dependent on the surrounding polymer matrix, not on the aquaporin channels themselves. Although aquaporins have the potential to create highly permeable, salt-rejecting membranes, no studies to date have demonstrated higher performance data for aquaporin-based membranes than for state-of-the-art thin-film composite desalination membranes (*48*).

Although some initial fouling and cleaning data have been reported for aquaporin-based membranes (*49*), further exploration of the long-term robustness of such membranes in actual desalination processes is needed. Examples of such studies include fouling properties, tolerance to common membrane-cleaning chemistries, and stability of AQP-based membranes. Moreover, higher selectivity is needed to be competitive with existing RO membranes. Depending upon its source, water slated for desalination can contain complex mixtures of ions and other components, some of which (e.g., mercury ions) are known to disable water transport in aquaporins (*93*). Studies to date have mainly focused on simple salts (e.g., NaCl), so the performance of such membranes for separating other common ions, or mixtures of ions, is largely unknown. Ability to remove solutes such as boron and low molar mass neutral molecules, which are problematic for existing RO membranes, has not been reported. Similar considerations will apply to other biomimetic membrane structures under development.

Design constraints beyond permeability and selectivity

Many studies focus exclusively on making membrane materials with better permeability and/or better selectivity. However, the ultimate performance of a membrane is gauged by flux (or permeance) and ability to separate mixtures of practical interest. High flux depends on using high-permeability materials and making thin membranes from those materials, which is why the separating layer of current membranes is often less than 100 nm thick. Making such thin, defect-free membranes on a large scale in a reproducible fashion is a critical barrier to introduction of new membrane materials. Moreover, as discussed further below, not every separation demands or even benefits from membranes with ultrahigh permeability or selectivity. Additionally, some applications cannot use or benefit from higher flux. To date, only a handful of families of polymers have been commercialized as separation membranes (*3*). High permeability is one component of high flux but not the only one. To obtain high flux, one may design a material with a higher permeability coefficient, make an existing membrane thinner, or increase the driving force for transport. However, there are limitations and drawbacks to each of these approaches.

Figure 4 shows cross sections of typical gas separation and RO membranes. All membranes for these applications are formed in solvent-based processes that lead to a thin (~100 nm) selective membrane layer situated on a porous support, which provides mechanical strength to the thin selective membrane. This is about the thinnest that can be achieved in large-scale membrane production processes with current procedures without introducing intolerable amounts of pinhole defects (i.e., through pores) that allow selectivity-destroying bulk convective flow (*74*, *75*). The porous support may be 50 to 200 (or more) μm thick and typically has surface porosity values in the range of 1 to 10%, with small surface pores (<100 nm) to provide a relatively smooth surface for the nonporous selective layer (*99*, *100*).

Figure 5A shows an example of the effect of support mass transfer resistance on upper-bound performance of a thin-film composite (TFC) gas separation membrane consisting of a thin selective separating layer on top of a porous support. Such membrane structures are widely used commercially because the separation layer thickness can be quite thin (~100 nm) and, in many cases, the support can be made from a low-cost, mechanically robust engineering thermoplastic (e.g., polysulfone). This approach allows one to use potentially exotic, expensive materials for the separating layer, because so little of this material is used per square meter of membrane area that the overall cost of the membrane can be quite low. However, if the thin selective layer becomes extremely thin (i.e., much less than 100 nm), the distance a solute molecule must travel through the selective layer of the membrane to reach a pore in the porous support can become greater than the selective layer thickness, and flux does not increase as expected with decreasing thickness. In gas separation membranes, addition of a high-permeability, thin "gutter" layer between the thin selective separating layer and the porous support helps mitigate this phenomenon, but simply making thinner selective layers does not guarantee flux increases (*99*). Although the porous support is often assumed to contribute negligibly to mass transfer resistance across a membrane (i.e., all of the mass transfer resistance is due to the thin selective membrane itself), this approximation becomes less and less valid as membrane materials become thinner and more permeable, leading to fluxes that do not increase as the thickness of the thin selective membrane decreases and selectivities that are far below intrinsic values of the separation material of interest (*101*). Thus, design of new membrane materials without consideration of membrane support properties can

lead to performance much worse than that expected based on results from free-standing films. Such support mass transfer resistance has been recognized, for example, to have pronounced performance-limiting effects in the current generation of forward osmosis membranes (*40*) and has long been important in gas separation membranes (*99*).

In water purification membranes, RO desalination provides an example of the insignificance of high-permeability membranes on process efficiency. Numerous studies have suggested that developing high-permeance RO membranes could reduce energy consumption in desalination, which is proportional to the applied hydraulic pressure to drive water permeation across the membrane (*1*, *72*, *96*). However, energy consumption is constrained by the conventional single-stage operation of RO systems, in which the minimum hydraulic pressure, and hence the minimum specific energy (i.e., energy per volume of product water), is equal to the osmotic pressure of the exiting brine (*1*, *102*). Recent process modeling for RO seawater desalination indicates that increasing membrane water permeance from 2 L m^{-2} h^{-1} bar^{-1}, the current level of commercial TFC desalination membranes, to 10 L m^{-2} h^{-1} bar^{-1}, results in only a 3.7% reduction in energy consumption (*102*). Moreover, a further 10-fold increase in permeance from 10 to 100 L m^{-2} h^{-1} bar^{-1} produces a meager 1.0% reduction in energy consumption. Similar conclusions were obtained when modeling RO brackish water desalination (*102*). Although high-permeance RO membranes may have the potential to reduce required membrane area, this solution will not be practical because severe concentration polarization (CP) induced by the high water flux will significantly hinder process performance (*1*). In addition, membrane fouling, which is already a major problem with current-generation membranes, is exacerbated at higher water fluxes (*103*, *104*). Rather than increasing membrane permeance, increasing the water-solute selectivity (or minimizing solute passage) of RO membranes should be a very important goal for improving process performance and yielding higher-quality product water (*48*, *102*). Current challenges with existing membranes include the removal of boron in seawater desalination, minimization of the passage of low–molecular weight toxic contaminants in water and wastewater reuse [e.g., arsenic, fluoride, and many uncharged solutes, such as endocrine disruptors increasingly found in water (*105*)], and production of high-purity water for various industries with minimal deionization steps after the RO stage (*102*).

Membrane separations are often limited by available driving force, so increases in membrane material selectivity result in little or no gain in product purity (*3*). In gas separation membranes, this concept is quantified by the pressure ratio (i.e., the ratio of feed to permeate pressure) divided by membrane selectivity (*3*). Pressure ratios may be set by economic considerations largely dependent on process conditions (i.e., independent of membrane properties). In gas separation applications, typical pressure ratios are 5 to 15 (*106*). Designing materials with selectivity values much greater than the pressure ratio yields little or no improvement in product purity, as shown in Fig. 5B. Membranes used in industrial hydrogen separations (*3*) and those considered for postcombustion carbon capture, for example, have low pressure ratios, limiting the need for highly selective membranes (*106*). Wessling and colleagues recently demonstrated the use of upper-bound properties of membranes coupled with process modeling to identify economically optimal combinations of permeability and selectivity for nitrogen removal from natural gas (*107*). Such studies for other gas and liquid separations of interest would be desirable to provide appropriate targets for materials design.

In addition to having excellent transport properties, membrane materials must be mechanically robust to survive manufacturing, installation, and long-term use. For example, seawater RO membranes are routinely used at pressures of 55 bar, and gas separation membranes may operate at

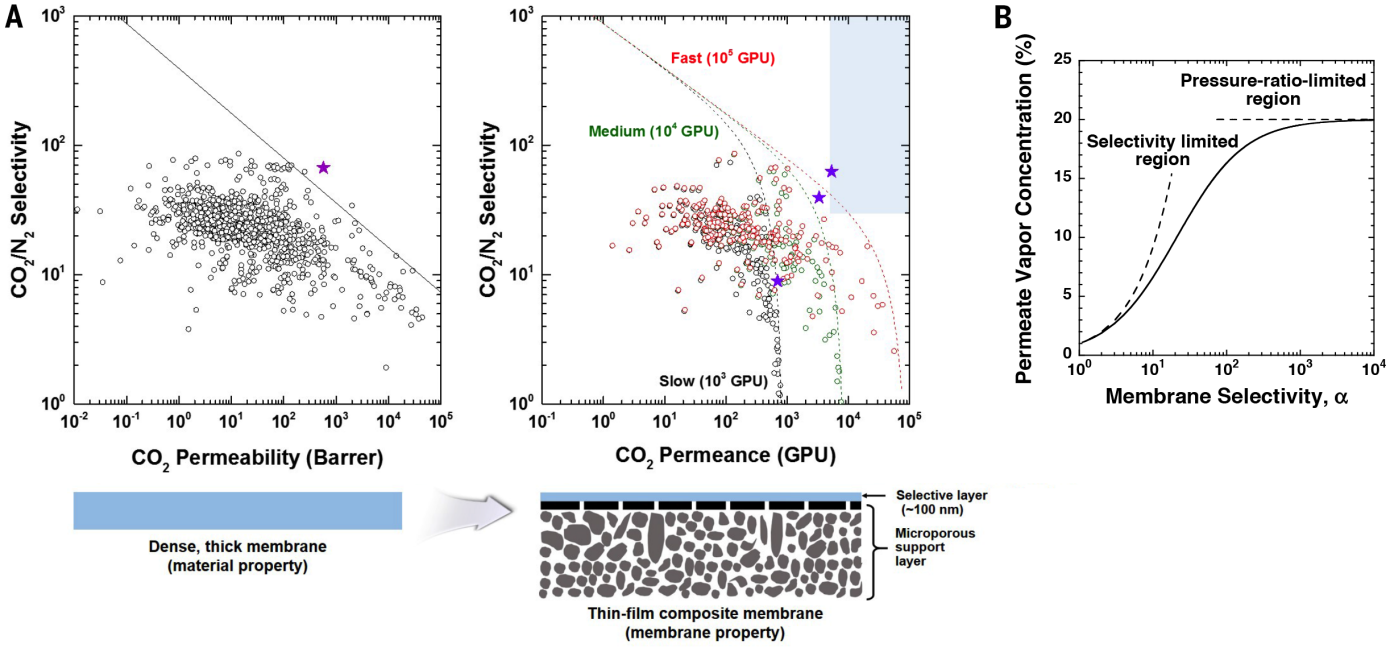

Fig. 5. Effect of membrane support and operating conditions on separation characteristics of gas separation membranes. (**A**) Membrane support. (**B**) operating conditions. (A) shows the 2008 upper-bound data for CO_2/N_2 separation translated into the selectivity and permeance (i.e., pressure-normalized flux) that could be achieved by placing a thin (100 nm) membrane onto a slow (10^3 GPU), medium (10^4 GPU), or fast (10^5 GPU) porous support membrane. For brevity, only 20% of the 2008 upper-bound data have been shown on the selectivity-permeance plot. The dashed lines indicate the expected performance of materials lying on the upper bound. The star [left side of (A)] denotes permeability/selectivity of a hypothetical material with separation properties above the upper bound. The stars [right side of (A)] denote permeance and selectivity of thin-film composite membranes of this material using different supports, showing that a high flux support is needed to reach desirable performance (blue shaded region) for postcombustion CO_2 capture (*15*). The procedure for generating the upper-bound lines in the selectivity-permeance plot is described here (*119*). (B) shows the effect of varying membrane selectivity on permeate vapor concentration for a vapor separation membrane operating at a feed/permeate pressure ratio of 20 and 1% vapor in the feed.

pressures exceeding 100 bar (*3*). High-salinity brines (e.g., much greater than seawater, such as water produced from hydraulic fracking) would require mechanically more robust RO membranes to enable operation at ultrahigh pressures. For example, using the extremely saline water (34% salinity) from the Dead Sea would require membranes operating at pressures of more than 250 bar (*108*). Details of the mechanical property requirements and design criteria, both for membranes and for their porous supports, are currently poorly understood, in part due to the lack of mechanical property data accompanying reports of new membrane materials.

Membrane materials must also be chemically and thermally tolerant to conditions encountered during operation. For example, oxidatively stable (i.e., chlorine tolerant) RO membranes remain an elusive goal. Such materials are needed because aqueous chlorine (e.g., hypochlorite) is widely used to control biological activity in water streams being fed to desalination processes, and current aromatic polyamide–based polymers, the state of the art for desalination membranes, have poor chlorine tolerance (*109*). Polymeric gas separation membranes are rarely deployed in applications exceeding 100°C due to a lack of stability of such membranes at high temperatures. Separations such as those found in precombustion carbon capture could benefit from membranes with much better thermal stability (*110*). Designing membranes that are resistant to plasticization (i.e., penetrant-induced swelling and subsequent loss of separation properties) will be required for membranes to be used in applications such as olefin/paraffin separation (*36*, *37*). Most important, membrane materials must be scalable to be manufactured in defect-free, large surface areas.

Outlook

Increasing demand for energy-efficient gas and water separations, coupled with growing availability of nanomaterials and a deeper understanding of the structural features of biological membranes that give them excellent permeability and selectivity, has stimulated substantial research aimed at overcoming the permeability/selectivity trade-off. Membranes in use today were discovered, in many cases, by serendipity. Molecular-level design and insight, including advanced simulation and modeling, will be critical for breakthroughs going forward. For example, the approaches used to prepare membranes today do not allow for independent control of permeation properties of interest [e.g., water transport cannot be controlled independent of salt (or other solute) transport, and the transport of one gas, e.g., CO_2, cannot be systematically manipulated without changing the transport of other gases, e.g., CH_4], even though such properties would be highly desirable. Whereas traditional membranes for water and gas separations are largely based on polymers and are subject to the permeability-selectivity trade-off, many new materials and design approaches (e.g., bioinspired, biomimetic, or MMMs) offer the hope of better control over pore size and size distribution, which can break the conventional upper bound.

However, many questions remain about both new and existing membranes. For example, our fundamental understanding of the basic thermodynamics and diffusion properties of water and ions in polymers used in RO and electrodialysis membranes and many energy applications (e.g., fuel cells, batteries, and reverse electrodialysis) is at an extremely rudimentary level (*111*), although recent advances in this area are allowing for prediction of ion sorption and transport in highly charged ion exchange membranes (*111*, *112*). While theoretical models have been proposed for the upper bound for gas separation membranes (*22*) and desalination membranes (*47*), no such analog exists today for other separations, such as electrodialysis, although the empirical evidence is overwhelming that such a trade-off exists (*46*). There is a real need for fundamental modeling, at length scales ranging from atomistic to continuum, to provide rational guidance for designing future membranes. More recently developed nanomaterials and MMMs would also benefit from an increased focus on fundamental modeling. In all cases, better understanding of structure-property-performance relationships in new, as well as existing, membrane materials is urgently needed.

For all membrane materials, it is critical to consider factors other than permeability and selectivity in materials design. Today, we typically use rather elaborate, nonequilibrium, continuous processes involving large amounts of volatile, potentially toxic solvents to manufacture membranes. An advantage to this approach is the widespread use of composite membranes, where a thin (~100 nm) separating membrane is applied to a porous support membrane, which can be made of a relatively inexpensive engineering thermoplastic. Such composite membranes allow the use of novel, expensive materials as the separating membrane, because so little of the separating membrane is required for a given area of membrane. Nevertheless, novel processing strategies to simplify membrane manufacturing and scale-up would contribute remarkably to accelerating deployment of new membrane materials. Development of solvent-free membrane manufacturing processes or processes using environmentally benign, inexpensive solvents (e.g., water) would bring about disruptive, sustainable changes in membrane fabrication. Issues such as process constraints, material processability, and long-term stability in the process environment where the membranes will operate should be built into research efforts to identify, as early as possible, materials that can be deployed for large-scale, practical challenges, such as the growing need for clean water, treatment of waste products from hydraulic fracturing, and climate change.

REFERENCES AND NOTES

1. M. Elimelech, W. A. Phillip, The future of seawater desalination: Energy, technology, and the environment. *Science* **333**, 712–717 (2011). doi: 10.1126/science.1200488; pmid: 21817042
2. M. A. Shannon *et al*., Science and technology for water purification in the coming decades. *Nature* **452**, 301–310 (2008). doi: 10.1038/nature06599; pmid: 18354474
3. R. W. Baker, *Membrane Technology and Applications* (John Wiley & Sons, Inc., ed. 3, Hoboken, NJ, 2012).
4. R. van Reis, A. Zydney, Bioprocess membrane technology. *J. Membr. Sci.* **297**, 16–50 (2007). doi: 10.1016/j.memsci.2007.02.045
5. H. Lutz, *Ultrafiltration for Bioprocessing: Development and Implementation of Robust Processes* (Elsevier, Amsterdam, 2015).
6. D. F. Stamatialis *et al*., Medical applications of membranes: Drug delivery, artificial organs and tissue engineering. *J. Membr. Sci.* **308**, 1–34 (2008). doi: 10.1016/j.memsci.2007.09.059
7. K.-V. Peinemann, S. P. Nunes, L. Giorno, *Membrane Technology: Volume 3: Membranes for Food Applications* (Wiley-VCH, Weinheim, Germany, 2010).
8. T. Sata, *Ion Exchange Membranes: Preparation, Characterization, Modification and Application* (Royal Society of Chemistry, London, 2004).
9. P. Arora, Z. J. Zhang, Battery separators. *Chem. Rev.* **104**, 4419–4462 (2004). doi: 10.1021/cr020738u; pmid: 15669158
10. S. J. Peighambardoust, S. Rowshanzamir, M. Amjadi, Review of the proton exchange membranes for fuel cell applications. *Int. J. Hydrogen Energy* **35**, 9349–9384 (2010). doi: 10.1016/j.ijhydene.2010.05.017
11. Y. Wang, K. S. Chen, J. Mishler, S. C. Cho, X. C. Adroher, A review of polymer electrolyte membrane fuel cells: Technology, applications, and needs on fundamental research. *Appl. Energy* **88**, 981–1007 (2011). doi: 10.1016/j.apenergy.2010.09.030
12. J. W. Post, H. V. M. Hamelers, C. J. N. Buisman, Energy recovery from controlled mixing salt and fresh water with a reverse electrodialysis system. *Environ. Sci. Technol.* **42**, 5785–5790 (2008). doi: 10.1021/es8004317; pmid: 18754509
13. B. E. Logan, M. Elimelech, Membrane-based processes for sustainable power generation using water. *Nature* **488**, 313–319 (2012). doi: 10.1038/nature11477; pmid: 22895336
14. R. S. Kingsbury, K. Chu, O. Coronell, Energy storage by reversible electrodialysis: The concentration battery. *J. Membr. Sci.* **495**, 502–516 (2015). doi: 10.1016/j.memsci.2015.06.050
15. T. C. Merkel, H. Lin, X. Wei, R. Baker, Power plant post-combustion carbon dioxide capture: An opportunity for membranes. *J. Membr. Sci.* **359**, 126–139 (2010). doi: 10.1016/j.memsci.2009.10.041
16. L. M. Blaney, S. Cinar, A. K. SenGupta, Hybrid anion exchanger for trace phosphate removal from water and wastewater. *Water Res.* **41**, 1603–1613 (2007). doi: 10.1016/j.watres.2007.01.008; pmid: 17306856
17. L. S. White, Development of large-scale applications in organic solvent nanofiltration and pervaporation for chemical and refining processes. *J. Membr. Sci.* **286**, 26–35 (2006). doi: 10.1016/j.memsci.2006.09.006
18. P. Marchetti, M. F. Jimenez Solomon, G. Szekely, A. G. Livingston, Molecular separation with organic solvent nanofiltration: A critical review. *Chem. Rev.* **114**, 10735–10806 (2014). doi: 10.1021/cr500006j; pmid: 25333504
19. E. Curcio, E. Drioli, Membrane distillation and related operations: A review. *Separ. Purif. Rev.* **34**, 35–86 (2005). doi: 10.1081/SPM-200054951
20. S. M. Joscelyne, G. Trägårdh, Membrane emulsification: A literature review. *J. Membr. Sci.* **169**, 107–117 (2000). doi: 10.1016/S0376-7388(99)00334-8
21. L. M. Robeson, Correlation of separation factor versus permeability for polymeric membranes. *J. Membr. Sci.* **62**, 165–185 (1991). doi: 10.1016/0376-7388(91)80060-J
22. B. D. Freeman, Basis of permeability/selectivity tradeoff relations in polymeric gas separation membranes. *Macromolecules* **32**, 375–380 (1999). doi: 10.1021/ma9814548
23. L. M. Robeson, The upper bound revisited. *J. Membr. Sci.* **320**, 390–400 (2008). doi: 10.1016/j.memsci.2008.04.030
24. W. Song, P. J. Rossky, M. Maroncelli, Modeling alkane+perfluoroalkane interactions using all-atom potentials: Failure of the usual combining rules. *J. Chem. Phys.* **119**, 9145–9162 (2003). doi: 10.1063/1.1610435
25. T. C. Merkel, I. Pinnau, R. Prabhakar, B. D. Freeman, in *Materials Science of Membranes*, Y. Yampolskii, I. Pinnau, B. D. Freeman, Eds. (John Wiley & Sons Ltd., Chichester, UK, 2006), pp. 251–270.

26. P. M. Budd, N. B. McKeown, D. Fritsch, Free volume and intrinsic microporosity in polymers. *J. Mater. Chem.* **15**, 1977 (2005). doi: 10.1039/b417402j
27. H. B. Park *et al.*, Polymers with cavities tuned for fast selective transport of small molecules and ions. *Science* **318**, 254–258 (2007). doi: 10.1126/science.1146744; pmid: 17932294
28. L. M. Robeson, M. E. Dose, B. D. Freeman, D. R. Paul, Analysis of the transport properties of thermally rearranged (TR) polymers and polymers of intrinsic microporosity (PIM) relative to upper bound performance. *J. Membr. Sci.* **525**, 18–24 (2017). doi: 10.1016/j.memsci.2016.11.085
29. L. M. Robeson, Q. Liu, B. D. Freeman, D. R. Paul, Comparison of transport properties of rubbery and glassy polymers and the relevance to the upper bound relationship. *J. Membr. Sci.* **476**, 421–431 (2015). doi: 10.1016/j.memsci.2014.11.058
30. D. F. Sanders *et al.*, Energy-efficient polymeric gas separation membranes for a sustainable future: A review. *Polymer (Guildf.)* **54**, 4729–4761 (2013). doi: 10.1016/j.polymer.2013.05.075
31. I. K. Meier, M. Langsam, H. C. Klotz, Selectivity enhancement via photooxidative surface modification of polyimide air separation membranes. *J. Membr. Sci.* **94**, 195–212 (1994). doi: 10.1016/0376-7388(93)E0174-I
32. C. H. Park *et al.*, Nanocrack-regulated self-humidifying membranes. *Nature* **532**, 480–483 (2016). doi: 10.1038/nature17634; pmid: 27121841
33. H. Nishide, T. Suzuki, H. Kawakami, E. Tsuchida, Cobalt porphyrin-mediated oxygen transport in a polymer membrane: effect of the cobalt porphyrin structure on the oxygen-binding reaction, oxygen-diffusion constants, and oxygen-transport efficiency. *J. Phys. Chem.* **98**, 5084–5088 (1994). doi: 10.1021/j100070a023
34. L. M. Robeson, Polymer blends in membrane transport processes. *Ind. Eng. Chem. Res.* **49**, 11859–11865 (2010). doi: 10.1021/ie100153q
35. C. M. Zimmerman, A. Singh, W. J. Koros, Tailoring mixed matrix composite membranes for gas separations. *J. Membr. Sci.* **137**, 145–154 (1997). doi: 10.1016/S0376-7388(97)00194-4
36. R. L. Burns, W. J. Koros, Defining the challenges for C_3H_6/C_3H_8 separation using polymeric membranes. *J. Membr. Sci.* **211**, 299–309 (2003). doi: 10.1016/S0376-7388(02)00430-1
37. M. Rungta, C. Zhang, W. J. Koros, L. Xu, Membrane-based ethylene/ethane separation: The upper bound and beyond. *AIChE J.* **59**, 3475–3489 (2013). doi: 10.1002/aic.14105
38. S. Park *et al.*, The polymeric upper bound for N_2/NF_3 separation and beyond; ZIF-8 containing mixed matrix membranes. *J. Membr. Sci.* **486**, 29–39 (2015). doi: 10.1016/j.memsci.2015.03.030
39. G. M. Geise, H. B. Park, A. C. Sagle, B. D. Freeman, J. E. McGrath, Water permeability and water/salt selectivity tradeoff in polymers for desalination. *J. Membr. Sci.* **369**, 130–138 (2011). doi: 10.1016/j.memsci.2010.11.054
40. D. L. Shaffer, J. R. Werber, H. Jaramillo, S. Lin, M. Elimelech, Forward osmosis: Where are we now? *Desalination* **356**, 271–284 (2015). doi: 10.1016/j.desal.2014.10.031
41. N. Y. Yip *et al.*, Thin-film composite pressure retarded osmosis membranes for sustainable power generation from salinity gradients. *Environ. Sci. Technol.* **45**, 4360–4369 (2011). doi: 10.1021/es104325z; pmid: 21491936
42. J. Wei, X. Liu, C. Qiu, R. Wang, C. Y. Tang, Influence of monomer concentrations on the performance of polyamide-based thin film composite forward osmosis membranes. *J. Membr. Sci.* **381**, 110–117 (2011). doi: 10.1016/j.memsci.2011.07.034
43. A. Mehta, A. L. Zydney, Permeability and selectivity analysis for ultrafiltration membranes. *J. Membr. Sci.* **249**, 245–249 (2005). doi: 10.1016/j.memsci.2004.09.040
44. L. Robeson, H. Hwu, J. McGrath, Upper bound relationship for proton exchange membranes: Empirical relationship and relevance of phase separated blends. *J. Membr. Sci.* **302**, 70–77 (2007). doi: 10.1016/j.memsci.2007.06.029
45. C. P. Ribeiro, B. D. Freeman, D. S. Kalika, S. Kalakkunnath, Aromatic polyimide and polybenzoxazole membranes for the fractionation of aromatic/aliphatic hydrocarbons by pervaporation. *J. Membr. Sci.* **390-391**, 182–193 (2012). doi: 10.1016/j.memsci.2011.11.042
46. G. M. Geise, M. A. Hickner, B. E. Logan, Ionic resistance and permselectivity tradeoffs in anion exchange membranes. *ACS Appl. Mater. Interfaces* **5**, 10294–10301 (2013). doi: 10.1021/am403207w; pmid: 24040962
47. H. Zhang, G. M. Geise, Modeling the water permeability and water/salt selectivity tradeoff in polymer membranes. *J. Membr. Sci.* **520**, 790–800 (2016). doi: 10.1016/j.memsci.2016.08.035
48. J. R. Werber, C. O. Osuji, M. Elimelech, Materials for next-generation desalination and water purification membranes. *Nat. Rev. Mater.* **1**, 16018 (2016). doi: 10.1038/natrevmats.2016.18
49. X. Li *et al.*, Nature gives the best solution for desalination: Aquaporin-based hollow fiber composite membrane with superior performance. *J. Membr. Sci.* **494**, 68–77 (2015). doi: 10.1016/j.memsci.2015.07.040
50. S. Y. Yang *et al.*, Nanoporous membranes with ultrahigh selectivity and flux for the filtration of viruses. *Adv. Mater.* **18**, 709–712 (2006). doi: 10.1002/adma.200501500
51. K. V. Peinemann, V. Abetz, P. F. Simon, Asymmetric superstructure formed in a block copolymer via phase separation. *Nat. Mater.* **6**, 992–996 (2007). doi: 10.1038/nmat2038; pmid: 17982467
52. X. Qiu *et al.*, Selective separation of similarly sized proteins with tunable nanoporous block copolymer membranes. *ACS Nano* **7**, 768–776 (2013). doi: 10.1021/nn305073e; pmid: 23252799
53. H. Yu *et al.*, Self-assembled asymmetric block copolymer membranes: Bridging the gap from ultra- to nanofiltration. *Angew. Chem. Int. Ed.* **54**, 13937–13941 (2015). doi: 10.1002/anie.201505663; pmid: 26388216
54. V. Abetz, Isoporous block copolymer membranes. *Macromol. Rapid Commun.* **36**, 10–22 (2015). doi: 10.1002/marc.201400556; pmid: 25451792
55. J. E. Bachman, Z. P. Smith, T. Li, T. Xu, J. R. Long, Enhanced ethylene separation and plasticization resistance in polymer membranes incorporating metal-organic framework nanocrystals. *Nat. Mater.* **15**, 845–849 (2016). doi: 10.1038/nmat4621; pmid: 27064528
56. H. Furukawa, K. E. Cordova, M. O'Keeffe, O. M. Yaghi, The chemistry and applications of metal-organic frameworks. *Science* **341**, 1230444 (2013). doi: 10.1126/science.1230444; pmid: 23990564
57. B. R. Pimentel, A. Parulkar, E. K. Zhou, N. A. Brunelli, R. P. Lively, Zeolitic imidazolate frameworks: Next-generation materials for energy-efficient gas separations. *ChemSusChem* **7**, 3202–3240 (2014). doi: 10.1002/cssc.201402647; pmid: 25363474
58. A. J. Brown *et al.*, Separation membranes. Interfacial microfluidic processing of metal-organic framework hollow fiber membranes. *Science* **345**, 72–75 (2014). doi: 10.1126/science.1251181; pmid: 24994649
59. D. S. Sholl, R. P. Lively, Defects in metal-organic frameworks: Challenge or opportunity? *J. Phys. Chem. Lett.* **6**, 3437–3444 (2015). doi: 10.1021/acs.jpclett.5b01135; pmid: 26268796
60. H. T. Kwon, H. K. Jeong, A. S. Lee, H. S. An, J. S. Lee, Heteroepitaxially grown zeolitic imidazolate framework membranes with unprecedented propylene/propane separation performances. *J. Am. Chem. Soc.* **137**, 12304–12311 (2015). doi: 10.1021/jacs.5b06730; pmid: 26364888
61. V. Singh *et al.*, Graphene based materials: Past, present and future. *Prog. Mater. Sci.* **56**, 1178–1271 (2011). doi: 10.1016/j.pmatsci.2011.03.003
62. S. P. Koenig, L. Wang, J. Pellegrino, J. S. Bunch, Selective molecular sieving through porous graphene. *Nat. Nanotechnol.* **7**, 728–732 (2012). doi: 10.1038/nnano.2012.162; pmid: 23042491
63. H. W. Kim *et al.*, Selective gas transport through few-layered graphene and graphene oxide membranes. *Science* **342**, 91–95 (2013). doi: 10.1126/science.1236098; pmid: 24092738
64. S. P. Surwade *et al.*, Water desalination using nanoporous single-layer graphene. *Nat. Nanotechnol.* **10**, 459–464 (2015). doi: 10.1038/nnano.2015.37; pmid: 25799521
65. Dow FilmTec Seamaxx Element Product Data Sheet, http://msdssearch.dow.com/PublishedLiteratureDOWCOM/dh_0948/0901b80380948b83.pdf?filepath=liquidseps/pdfs/noreg/609-50126.pdf&fromPage=GetDoc (May 8, 2016).
66. M. Grzelakowski, M. F. Cherenet, Y. Shen, M. Kumar, A framework for accurate evaluation of the promise of aquaporin based biomimetic membranes. *J. Membr. Sci.* **479**, 223–231 (2015). doi: 10.1016/j.memsci.2015.01.023
67. D. Cohen-Tanugi, R. K. McGovern, S. H. Dave, J. H. Lienhard, J. C. Grossman, Quantifying the potential of ultra-permeable membranes for water desalination. *Energy Environ. Sci.* **7**, 1134–1141 (2014). doi: 10.1039/C3EE43221A
68. A state-of-the-art commercial RO membrane (Dow SEAMAXX 440i) has a reported water volumetric flow rate of 17,000 gallons per day through an active membrane area of 41 m^2 when operated as designed (i.e., feed salt concentration = 32,000 mg/L NaCl and feed pressure = 55.2 bar absolute) (65). The water flux through this membrane is approximately 65 L m^{-2} $hour^{-1}$. Normalizing for the driving force for water transport (i.e., $\Delta p - \Delta\pi = 55.2$ bar $-$ 27.1 bar $= 28.1$ bar), the permeance is 2.3 L m^{-2} $hour^{-1}$ bar^{-1}. The osmotic pressure difference, $\Delta\pi$, was calculated using the van't Hoff relation (i.e., π = CRT). The salt concentration in the permeate (96 mg/L) was calculated from the reported salt rejection (99.70%) and a feed salt concentration (32,000 mg/L) (65). Aquaporins are reported to transport water at rates of 3×10^9 molecules per second through pores that are 0.28 nm in diameter (93–95). Thus, the water flux through an aquaporin is 52×10^5 L m^{-2} $hour^{-1}$, nearly 5 orders of magnitude greater than that in the commercial RO membrane. This estimate accounts for water transport through a single aquaporin channel. Such channels, configured in a close-packed array, would have a packing density of 0.25% (66), so the maximum hypothetical flux through a flat sheet membrane comprising aquaporins at this packing density would be 1.3×10^4 L m^{-2} $hour^{-1}$, which is ~200 times as high as that of the commercial RO membrane. This calculation does not include effects of concentration polarization, support layer resistance, fouling, or other effects that would likely be observed in practice, so the value reported here should be used only to compare intrinsic permeation properties of the biological and synthetic membrane, not practically achievable fluxes of an aquaporin-based membrane, because effects ignored in this analysis would be limited in a real membrane based on such ultrapermeable materials (67).
69. R. K. Joshi *et al.*, Precise and ultrafast molecular sieving through graphene oxide membranes. *Science* **343**, 752–754 (2014). doi: 10.1126/science.1245711; pmid: 24531966
70. D. R. Dreyer, S. Park, C. W. Bielawski, R. S. Ruoff, The chemistry of graphene oxide. *Chem. Soc. Rev.* **39**, 228–240 (2010). doi: 10.1039/B917103G; pmid: 20023850
71. R. R. Nair, H. A. Wu, P. N. Jayaram, I. V. Grigorieva, A. K. Geim, Unimpeded permeation of water through helium-leak-tight graphene-based membranes. *Science* **335**, 442–444 (2012). doi: 10.1126/science.1211694; pmid: 22282806
72. J. K. Holt *et al.*, Fast mass transport through sub-2-nanometer carbon nanotubes. *Science* **312**, 1034–1037 (2006). doi: 10.1126/science.1126298; pmid: 16709781
73. H. Li *et al.*, Ultrathin, molecular-sieving graphene oxide membranes for selective hydrogen separation. *Science* **342**, 95–98 (2013). doi: 10.1126/science.1236686; pmid: 24092739
74. J. M. S. Henis, M. K. Tripodi, The developing technology of gas separating membranes. *Science* **220**, 11–17 (1983). doi: 10.1126/science.220.4592.11; pmid: 17736148
75. J. M. S. Henis, M. K. Tripodi, Composite hollow fiber membranes for gas separation: The resistance model approach. *J. Membr. Sci.* **8**, 233–246 (1981). doi: 10.1016/S0376-7388(00)82312-1
76. S. Husain, W. J. Koros, Mixed matrix hollow fiber membranes made with modified HSSZ-13 zeolite in polyetherimide polymer matrix for gas separation. *J. Membr. Sci.* **288**, 195–207 (2007). doi: 10.1016/j.memsci.2006.11.016
77. R. Adams *et al.*, in *Encyclopedia of Membrane Science and Technology*, E. M. V. Hoek, V. V. Tarabara, Eds. (John Wiley & Sons, Inc., Hoboken, NJ, 2013).
78. B. Seoane *et al.*, Metal-organic framework based mixed matrix membranes: A solution for highly efficient CO_2 capture? *Chem. Soc. Rev.* **44**, 2421–2454 (2015). doi: 10.1039/C4CS00437J; pmid: 25692487
79. T. T. Moore, W. J. Koros, Non-ideal effects in organic–inorganic materials for gas separation membranes. *J. Mol. Struct.* **739**, 87–98 (2005). doi: 10.1016/j.molstruc.2004.05.043
80. H. Ha, J. Park, K. Ha, B. D. Freeman, C. J. Ellison, Synthesis and gas permeability of highly elastic poly(dimethylsiloxane)/graphene oxide composite elastomers using telechelic polymers. *Polymer (Guildf.)* **93**, 53–60 (2016). doi: 10.1016/j.polymer.2016.04.016
81. H. Ha *et al.*, Gas permeation and selectivity of poly (dimethylsiloxane)/graphene oxide composite elastomer membranes. *J. Membr. Sci.* **518**, 131–140 (2016). doi: 10.1016/j.memsci.2016.06.028
82. G. Dong, H. Li, V. Chen, Challenges and opportunities for mixed-matrix membranes for gas separation. *J. Mater. Chem. A Mater. Energy Sustain.* **1**, 4610 (2013). doi: 10.1039/c3ta00927k

83. A. A. Gusev, O. Guseva, Rapid mass transport in mixed matrix nanotube/polymer membranes. *Adv. Mater.* **19**, 2672–2676 (2007). doi: 10.1002/adma.200602018
84. Y. Peng *et al*., Metal-organic framework nanosheets as building blocks for molecular sieving membranes. *Science* **346**, 1356–1359 (2014). doi: 10.1126/science.1254227; pmid: 25504718
85. T. Rodenas *et al*., Metal-organic framework nanosheets in polymer composite materials for gas separation. *Nat. Mater.* **14**, 48–55 (2015). doi: 10.1038/nmat4113; pmid: 25362353
86. J. Shen *et al*., Membranes with fast and selective gas-transport channels of laminar graphene oxide for efficient CO_2 capture. *Angew. Chem. Int. Ed. Engl.* **54**, 578–582 (2015). pmid: 25378197
87. D. A. Doyle *et al*., The structure of the potassium channel: Molecular basis of K^+ conduction and selectivity. *Science* **280**, 69–77 (1998). doi: 10.1126/science.280.5360.69; pmid: 9525859
88. J. E. McGrath, H. B. Park, B. D. Freeman, Chlorine resistant desalination membranes based on directly sulfonated poly (arylene ether sulfone) copolymers. *U.S. Patent 8,028,842*, (4 October 2011).
89. G. M. Geise, D. R. Paul, B. D. Freeman, Fundamental water and salt transport properties of polymeric materials. *Prog. Polym. Sci.* **39**, 1–42 (2014). doi: 10.1016/j.progpolymsci.2013.07.001
90. B. Hille, *Ion Channels of Excitable Membranes, Third Edition* (Sinauer Associates, Inc., Sunderland, MA, 2001).
91. G. M. Geise *et al*., Water purification by membranes: The role of polymer science. *J. Polym. Sci. Polym. Phys.* **48**, 1685–1718 (2010). doi: 10.1002/polb.22037
92. P. N. Pintauro, D. N. Bennlon, Mass transport of electrolytes in membranes. 2. Determination of NaCl equilibrium and transport parameters for nafion. *Ind. Eng. Chem. Res.* **23**, 234–243 (1984).
93. P. Agre, Aquaporin water channels (Nobel Lecture). *Angew. Chem. Int. Ed. Engl.* **43**, 4278–4290 (2004). doi: 10.1002/anie.200460804; pmid: 15368374
94. J. S. Jung, G. M. Preston, B. L. Smith, W. B. Guggino, P. Agre, Molecular structure of the water channel through aquaporin CHIP. The hourglass model. *J. Biol. Chem.* **269**, 14648–14654 (1994). pmid: 7514176
95. G. M. Preston, T. P. Carroll, W. B. Guggino, P. Agre, Appearance of water channels in Xenopus oocytes expressing red cell CHIP28 protein. *Science* **256**, 385–387 (1992). doi: 10.1126/science.256.5055.385; pmid: 1373524
96. M. Kumar, M. Grzelakowski, J. Zilles, M. Clark, W. Meier, Highly permeable polymeric membranes based on the incorporation of the functional water channel protein Aquaporin Z. *Proc. Natl. Acad. Sci. U.S.A.* **104**, 20719–20724 (2007). doi: 10.1073/pnas.0708762104; pmid: 18077364
97. H. Wang *et al*., Highly permeable and selective pore-spanning biomimetic membrane embedded with aquaporin Z. *Small* **8**, 1185–1190, 1125 (2012). doi: 10.1002/smll.201102120; pmid: 22378644
98. Y. Zhao *et al*., Synthesis of robust and high-performance aquaporin-based biomimetic membranes by interfacial polymerization-membrane preparation and RO performance characterization. *J. Membr. Sci.* **423-424**, 422–428 (2012). doi: 10.1016/j.memsci.2012.08.039
99. M. Kattula *et al*., Designing ultrathin film composite membranes: The impact of a gutter layer. *Sci. Rep.* **5**, 15016 (2015). doi: 10.1038/srep15016; pmid: 26456377
100. X. Lu, L. H. Arias Chavez, S. Romero-Vargas Castrillón, J. Ma, M. Elimelech, Influence of active layer and support layer surface structures on organic fouling propensity of thin-film composite forward osmosis membranes. *Environ. Sci. Technol.* **49**, 1436–1444 (2015). doi: 10.1021/es5044062; pmid: 25564877
101. I. Pinnau, J. G. Wijmans, I. Blume, T. Kuroda, K.-V. Peinemann, Gas permeation through composite membranes. *J. Membr. Sci.* **37**, 81–88 (1988). doi: 10.1016/S0376-7388(00)85070-X
102. J. R. Werber, A. Deshmukh, M. Elimelech, The critical need for increased selectivity, not increased water permeability, for desalination membranes. *Environ. Sci. Technol. Lett.* **3**, 112–120 (2016). doi: 10.1021/acs.estlett.6b00050
103. D. J. Miller, S. Kasemset, D. R. Paul, B. D. Freeman, Comparison of membrane fouling at constant flux and constant transmembrane pressure conditions. *J. Membr. Sci.* **454**, 505–515 (2014). doi: 10.1016/j.memsci.2013.12.027
104. R. Zhang *et al*., Antifouling membranes for sustainable water purification: Strategies and mechanisms. *Chem. Soc. Rev.* **45**, 5888–5924 (2016). doi: 10.1039/C5CS00579E; pmid: 27494001
105. S. A. Snyder *et al*., Role of membranes and activated carbon in the removal of endocrine disruptors and pharmaceuticals. *Desalination* **202**, 156–181 (2007). doi: 10.1016/j.desal.2005.12.052
106. Y. Huang, T. C. Merkel, R. W. Baker, Pressure ratio and its impact on membrane gas separation processes. *J. Membr. Sci.* **463**, 33–40 (2014). doi: 10.1016/j.memsci.2014.03.016
107. B. Ohs, J. Lohaus, M. Wessling, Optimization of membrane based nitrogen removal from natural gas. *J. Membr. Sci.* **498**, 291–301 (2016). doi: 10.1016/j.memsci.2015.10.007
108. A. P. Straub, A. Deshmukh, M. Elimelech, Pressure-retarded osmosis for power generation from salinity gradients: Is it viable? *Energy Environ. Sci.* **9**, 31–48 (2016). doi: 10.1039/C5EE02985F
109. H. B. Park, B. D. Freeman, Z. B. Zhang, M. Sankir, J. E. McGrath, Highly chlorine-tolerant polymers for desalination. *Angew. Chem. Int. Ed. Engl.* **47**, 6019–6024 (2008). doi: 10.1002/anie.200800454; pmid: 18604786
110. T. C. Merkel, M. Zhou, R. W. Baker, Carbon dioxide capture with membranes at an IGCC power plant. *J. Membr. Sci.* **389**, 441–450 (2012). doi: 10.1016/j.memsci.2011.11.012
111. J. Kamcev *et al*., Partitioning of mobile ions between ion exchange polymers and aqueous salt solutions: Importance of counter-ion condensation. *Phys. Chem. Chem. Phys.* **18**, 6021–6031 (2016). doi: 10.1039/C5CP06747B; pmid: 26840776
112. J. Kamcev, D. R. Paul, G. S. Manning, B. D. Freeman, Predicting salt permeability coefficients in highly swollen, highly charged ion exchange membranes. *ACS Appl. Mater. Interfaces* **9**, 4044–4056 (2017). doi: 10.1021/acsami.6b14902; pmid: 28072514
113. M. L. Greenfield, D. N. Theodorou, Geometric analysis of diffusion pathways in glassy and melt atactic polypropylene. *Macromolecules* **26**, 5461–5472 (1993). doi: 10.1021/ma00072a026
114. S. R. Wickramasinghe, S. E. Bower, Z. Chen, A. Mukherjee, S. M. Husson, Relating the pore size distribution of ultrafiltration membranes to dextran rejection. *J. Membr. Sci.* **340**, 1–8 (2009). doi: 10.1016/j.memsci.2009.04.056
115. J. Bai, X. Zhong, S. Jiang, Y. Huang, X. Duan, Graphene nanomesh. *Nat. Nanotechnol.* **5**, 190–194 (2010). doi: 10.1038/nnano.2010.8; pmid: 20154685
116. J. H. Morais-Cabral, Y. Zhou, R. MacKinnon, Energetic optimization of ion conduction rate by the K^+ selectivity filter. *Nature* **414**, 37–42 (2001). doi: 10.1038/35102000; pmid: 11689935
117. S. Gravelle *et al*., Optimizing water permeability through the hourglass shape of aquaporins. *Proc. Natl. Acad. Sci. U.S.A.* **110**, 16367–16372 (2013). doi: 10.1073/pnas.1306447110; pmid: 24067650
118. L. Liu, E. S. Sanders, S. S. Kulkarni, D. J. Hasse, W. J. Koros, Sub-ambient temperature flue gas carbon dioxide capture via Matrimid® hollow fiber membranes. *J. Membr. Sci.* **465**, 49–55 (2014). doi: 10.1016/j.memsci.2014.03.060
119. The gas permeance of a thin film composite membrane, J_c, can be calculated using the series resistance model (*10*) $1/J_c = \ell_A/P_A + 1/J_B$, where P_A is the gas permeability (in units of barrer) of the active layer, J_B is the gas permeance (in units of GPU) of the porous support, and ℓ_A is the thickness of the separation membrane (i.e., active layer). The permeance-selectivity data in Fig. 4A were calculated using this model. The CO_2 permeance of the composite membrane was calculated from $J_c^{CO_2} = (\ell_A/P_A^{CO_2} + 1/J_B^{CO_2})^{-1}$ and the N_2 permeance of the composite membrane was calculated from $J_c^{N_2} = (\ell_A/P_A^{N_2} + 1/J_B^{N_2})^{-1}$. Finally, the selectivity, $\alpha^C_{CO_2/N_2}$, was calculated from $\alpha^C_{CO_2/N_2} = J_c^{CO_2}/J_c^{N_2}$. To demonstrate the importance of the porous support layer, the N_2 permeance of the porous support layer in Fig. 4A is varied over a range of values (1000, 10,000, and 100,000 GPU) representing slow, medium, and fast support membranes, respectively. Assuming Knudsen selectivity in the porous support, the CO_2 permeance of the porous support layer is then calculated from $J_B^{CO_2} = J_B^{N_2}\sqrt{M_{N_2}/M_{CO_2}} = 0.798J_B^{N_2}$, where M_{N_2} is the molecular mass of N_2, and M_{CO_2} is the molecular mass of CO_2. The dashed lines in the selectivity-permeance plot in Fig. 4A were generated as described below. The upper-bound relationship for CO_2/N_2 is (*23*) $P_{CO_2} = 30,967,000(\alpha_{CO_2/N_2})^{-2.888}$. This equation was used to obtain CO_2/N_2 selectivities for CO_2 permeability values ranging from 10^{-4} to 10^5 barrer. Subsequently, N_2 permeability values were calculated from $P_{N_2} = P_{CO_2}/\alpha_{CO_2/N_2}$. The selectivity and permeance values for the composite membranes were then calculated according to procedures described above.
120. J. G. Wijmans, R. W. Baker, The solution-diffusion model: A review. *J. Membr. Sci.* **107**, 1–21 (1995). doi: 10.1016/0376-7388(95)00102-I
121. D. R. Paul, Reformulation of the solution-diffusion theory of reverse osmosis. *J. Membr. Sci.* **241**, 371–386 (2004). doi: 10.1016/j.memsci.2004.05.026

ACKNOWLEDGMENTS

We are grateful to many members of the membrane community worldwide who contributed articles, advice, and perspectives during the preparation of this review. H.B.P and B.D.F. acknowledge financial support by the Korea CCS R&D Center (KCRC) grant funded by Ministry of Science, ICT, and Future Planning from the Korean government (grant 2016910057). The work of J.K. and B.D.F. was supported by the Australian-American Fulbright Commission for the award to B.D.F. of the U.S. Fulbright Distinguished Chair in Science, Technology, and Innovation sponsored by the Commonwealth Scientific and Industrial Research Organization (CSIRO); the Division of Chemical Sciences, Geosciences, and Biosciences, Office of Basic Energy Sciences of the U.S. Department of Energy (grant DE-FG02-02ER15362); and the International Institute for Carbon Neutral Energy Research (WPI-I2CNER), sponsored by the World Premier International Research Center Initiative (WPI), MEXT, Japan. The work of J.K. was also sponsored by the National Science Foundation (NSF) Graduate Research Fellowship under grant DGE-1110007. The work of M.E. was supported by the National Science Foundation through the Engineering Research Center for Nanotechnology-Enabled Water Treatment (ERC-1449500) and by grant CBET 1437630. We also thank E. Zumalt and P. Wiseman for preparing the graphic for the print summary.

10.1126/science.aab0530

Maximizing the right stuff: The trade-off between membrane permeability and selectivity

Ho Bum Park, Jovan Kamcev, Lloyd M. Robeson, Menachem Elimelech and Benny D. Freeman

Science **356** (6343), eaab0530.
DOI: 10.1126/science.aab0530

Filtering through to what's important

Membranes are widely used for gas and liquid separations. Historical analysis of a range of gas pair separations indicated that there was an upper bound on the trade-off between membrane permeability, which limits flow rates, and the selectivity, which limits the quality of the separation process. Park *et al.* review the advances that have been made in attempts to break past this upper bound. Some inspiration has come from biological membranes. The authors also highlight cases where the challenges lie in areas other than improved separation performance.

Science, this issue p. eaab0530